doi: 10.18323/2782-4039-2025-3-73-6

Study of the influence of deformation temperature on the mechanical behaviour and fracturing behaviour of the cast TNM-B1 alloy

Vitaly S. Sokolovskiy*, PhD (Engineering),
researcher of the Laboratory of Bulk Nanostructured Materials
Gennady A. Salishchev[1], Doctor of Sciences (Engineering), Professor,
Head of the Laboratory of Bulk Nanostructured Materials
Belgorod State University, Belgorod (Russia)

***E-mail:** sokolovskiy@bsuedu.ru [1]ORCID: https://orcid.org/0000-0002-0815-3525

Received 07.07.2025 *Revised 25.07.2025* *Accepted 20.08.2025*

Abstract: The paper covers the study of β-solidifying TiAl-based alloys, which are extremely promising materials for the aviation industry with an operating temperature of up to 850 °C, have high specific strength characteristics. The authors studied the influence of tensile deformation temperature in the range of T=25–1000 °C on the mechanical properties, phase composition and crack formation in the cast β-solidifying TNM-B1 alloy. It is found that the cast TNM-B1 alloy is characterized by a complex microstructure, including (α_2+γ) lamellar colonies and interlayers of β(B2)+ω phases, the evolution of which at elevated deformation temperatures determines the material behaviour. It is shown that the ω-phase dissolution and the precipitation of dispersed secondary β-phase particles at T>950 °C have a significant influence on the mechanical characteristics. A pronounced temperature dependence of strength and ductility is identified: the maximum strength is observed at 800 °C, while the greatest relative elongation in the studied temperature range is achieved at 1000 °C. The transition from brittle to viscous fracture occurs in the temperature range of about 950 °C. Moreover, a dependence of the crack propagation mechanism on the orientation of lamellar colonies relative to the deformation axis is revealed: with an increase in temperature, the differences are leveled, and at 1000 °C, complete suppression of crack formation with the formation of pores along the boundaries of colonies and clusters of secondary β-phase particles is observed. The obtained results demonstrate the important role of microstructural transformations in the formation of deformation behaviour and mechanical properties of the TNM-B1 alloy based on gamma-titanium aluminide, which is of practical importance for the development of technologies for its thermomechanical processing.

Keywords: TNM-B1 cast alloy; mechanical behaviour; fracturing behaviour; TNM alloy; microstructure; brittle-ductile transition; strength; plasticity.

Acknowledgments: The work was carried out with the financial support of the Russian Science Foundation (agreement No. 19-79-30066) using the equipment of the Common Use Center "Technologies and Materials" of BelSU National Research University, https://rscf.ru/prjcard_int?19-79-30066.

For citation: Sokolovskiy V.S., Salishchev G.A. Study of the influence of deformation temperature on the mechanical behaviour and fracturing behaviour of the cast TNM-B1 alloy. *Frontier Materials & Technologies*, 2025, no. 3, pp. 81–89. DOI: 10.18323/2782-4039-2025-3-73-6.

INTRODUCTION

Intermetallic alloys based on gamma-titanium aluminide (γ-TiAl) are considered as promising materials with an operating temperature of up to 850 °C for use in the aerospace and energy industries, where a combination of heat resistance, low density and oxidation resistance is required [1–3]. Among the γ-TiAl-based alloys, β-solidifying alloys, a typical representative of which is TNM-B1, are of particular interest [4]. The fundamental limitation of the application of γ-TiAl-based intermetallic alloys is their tendency to brittle fracture up to T=1000 °C [5–7], which is caused by the nature of the γ(TiAl-$L1_0$), α_2(Ti_3Al-$D0_{19}$) and β(B2) phases present in them, characterised by a limited number of active slip/twinning systems, reduced diffusion, difficult transmission of deformation across boundaries and, accordingly, pronounced deformation localisation [8; 9]. As the temperature increases above 650–850 °C, the number of slip/twinning systems increases, diffusion accelerates and dislocation climb is activated [10; 11]. The transition from the brittle to the ductile state also leads to a change in the type of fracture from intercrystallite to transcrystalline in the transition state and dimple in the case of ductile fracture [8]. The orientation of the plates relative to the deformation axis has a significant influence on the development of fracture. It was shown earlier [9; 12] that the orientation of lamellar colonies relative to the external load Φ largely determines their mechanical behaviour. Thus, colonies with an orientation of 15<Φ<75° relative to the loading axis are deformed first, in contrast

to colonies with Φ<15° and Φ>75°, in which significantly higher stresses are required to activate slip/twinning systems [12]. This feature should directly influence the propagation of cracks in colonies with different orientations relative to the deformation axis in alloys with a lamellar type of structure. Meanwhile, the effect of the orientation of lamellar colonies on the fracture development in the temperature range of the brittle-ductile transition (BDT) has not been considered in detail in the literature. It is worth noting that in addition to the above phases, TNM alloys may also contain ω(Ti_4Nb_3Al-$B8_2$)-phase particles, which are formed in the β-phase interlayers during slow cooling or holding below *T*=850 °C [13]. During subsequent heating, these particles dissolve, the proportion of the β-phase increases, and the γ-phase particles dissolve/spheroidise, which can significantly affect the fracturing behaviour in the temperature range corresponding to the brittle-ductile transition. However, the assessment of this effect has not been given due attention in the literature [1–3].

The aim of the work is to study the influence of the deformation temperature of cast β-solidifying TNM-B1 alloy with a lamellar structure on its mechanical properties, phase composition, and fracturing behaviour in colonies with different orientations relative to the deformation axis.

METHODS

The starting material was the TNM-B1 intermetallic alloy based on gamma-titanium aluminide with the nominal composition Ti–43.5Al–4Nb–1Mo–0.1B. An ingot with a diameter of 18 mm and a length of 90 mm was produced by die-casting. The chemical composition of the alloy ingot is presented in Table 1.

After mechanical grinding, the cast alloy samples for testing mechanical properties were additionally subjected to electrolytic polishing. An electrolyte of 95 % C_2H_5OH + 5 % HCl was used; the electrolytic polishing temperature was −35 °C, and the current density was 0.1 A/m^2.

Tensile tests were carried out to determine the mechanical properties. An Instron 5882 universal electromechanical testing machine (USA) equipped with a furnace with a maximum heating temperature of 1200 °C was used. The tests were carried out in the temperature range from 25 to 1000 °C. The deformation rate was 0.96 mm/min; the initial deformation rate was 10^{-3} s^{-1}. Flat samples with a length of the working part of 16 mm and a cross section of 1.5×3 mm were used. Only samples with visually no pores on the surface were selected for tensile testing.

The microstructure was analysed using a FEI Quanta 600 scanning electron microscope (USA) in the electron backscatter diffraction and secondary backscattered electron mode at an accelerating voltage of 30 kV. The fine structure of the alloy was studied using a JEOL JEM-2100 transmission electron microscope (Japan) at an accelerating voltage of 200 kV. For the research, foils with Ø3×0.1 mm were produced, which were subjected to electrolytic thinning on a TenuPol-5 device (Denmark), using electrolyte A2 from Struers (Denmark), the temperature was −32 °C, the voltage was 27 V.

RESULTS

Initial microstructure

During the SEM studies in the backscattered electron mode, images of the cast Ti–43.5Al–4.0Nb–1.0Mo–0.1B (TNM-B1) alloy microstructure were obtained; the higher the atomic number of the elements that make up the phases, the greater the image contrast (Fig. 1). It is seen that it is mainly represented by (α_2+γ) lamellar colonies, the proportion of which is 85 %, and their average size is 30 μm (Fig. 1 a). Analysis of the fine structure allowed identifying the average interlamellar distance equal to 120 nm (Fig. 1 b). Dark γ-phase particles and light layers of a mixture of β(B2)- and ω-phases were located along the boundaries of the colonies, which is confirmed by decoding the electron diffraction patterns from the areas of the corresponding particles (Fig. 1 b, c). The total volume fraction of β(B2)+ω-phases is 10 %, γ-phase – 5 %, the average particle size is 2 and 4 μm, respectively (Fig. 1 a, b). The whisker-shaped boride particles are mainly located along the colony boundaries and have an average length of about 15 μm with a diameter of 0.2 μm and a volume fraction of less than 0.1 % (Fig. 1 a). It is worth noting the presence of shrinkage pores in the alloy with a size from 1–10 to 50–100 μm with a volume fraction of 9 % and dark zones indicating the presence of liquation with a lower content of hard-melting elements (Nb, Mo) located mainly in the area of casting pores (Fig. 1 a).

Mechanical properties

The results of mechanical tensile tests in the temperature range of 25–1000 °C with an initial deformation rate of $\dot{\varepsilon}=10^{-3}$ s^{-1} are shown in Figs. 2, 3. It is evident that at *T*=25 °C, the cast alloy is destroyed in the elastic region. As the temperature increases to 700–800 °C, there is an increase in strength and some increase in ductility to δ=0.4 %. At *T*=900 °C, the strength decreases significantly, while the relative elongation reaches only 0.6 %.

Table 1. *Chemical composition of TNM-B1 alloy, at. %*
Таблица 1. *Химический состав сплава TNM-B1, ат. %*

Ti	Al	Nb	Mo	B
51.5	43.6	3.6	1.2	0.1

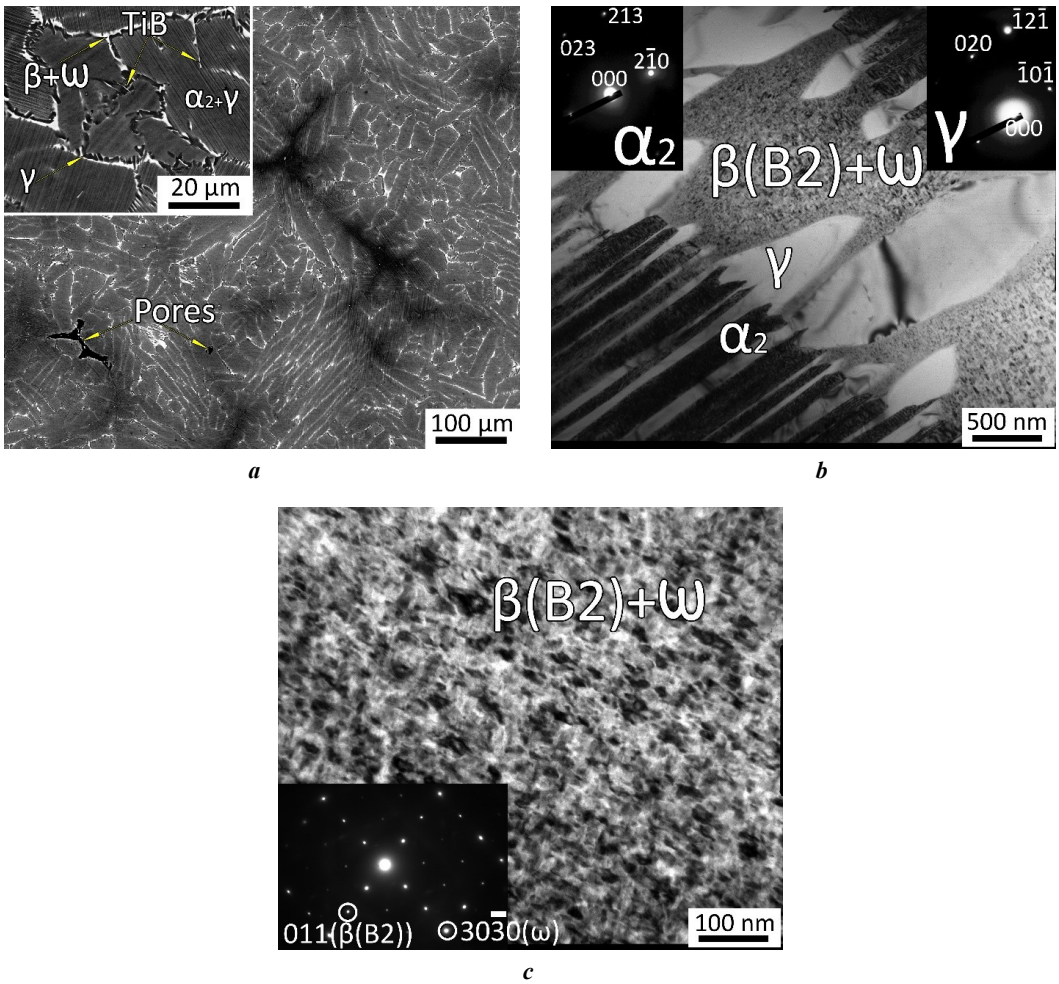

a *b*

c

Fig. 1. *Microstructure of the TNM-B1 alloy in the as-cast state: overview image and insert with high magnification (**a**), boundary of lamellar colonies (**b**), mixture of β(B2)+ω-phases (**c**).*
a *– SEM;* ***b***, ***c*** *– TEM with inserts of electron diffraction patterns of the corresponding phases.*
Arrows indicate the corresponding phases and structural elements
Рис. 1. *Микроструктура сплава TNM-B_1 в литом состоянии: обзорный снимок и вставка с большим увеличением (**a**), граница пластинчатых колоний (**b**), смесь β(B2)+ω-фаз (**c**).*
a *– СЭМ;* ***b***, ***c*** *– ПЭМ со вставками электронограмм соответствующих фаз.*
Стрелками обозначены соответствующие фазы и структурные элементы

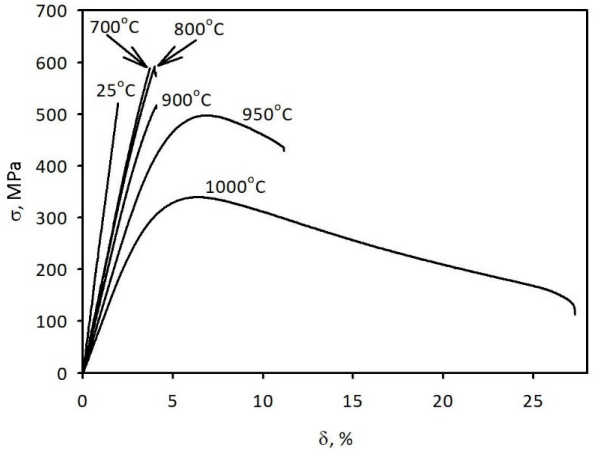

Fig. 2. *Stress-strain curves obtained during tensile testing of TNM-B1 alloy in the temperature range of 25–1000 °C ($\dot{\varepsilon} = 10^{-3}$ s^{-1})*
Рис. 2. *Кривые «напряжение – деформация», полученные при испытании на растяжение сплава TNM-B1 в интервале температур 25–1000 °C ($\dot{\varepsilon} = 10^{-3}$ c^{-1})*

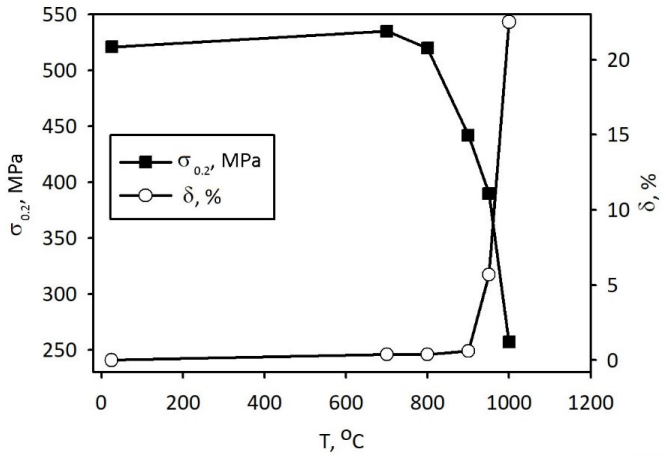

Fig. 3. *Dependences of the ultimate strength and relative elongation of cast TNM-B1 alloy on temperature*
Рис. 3. *Зависимости предела прочности и относительного удлинения литого сплава TNM-B1 от температуры*

Increasing the temperature to 950 °C leads to a decrease in the yield strength and a significant increase in ductility to δ=5.7 %. Increasing the deformation temperature to 1000 °C is accompanied by significant softening and an increase in the relative elongation to 22.5 %. Thus, it can be said that stretching at a temperature of 1000 °C corresponds to the viscous temperature range, 950 °C – to the transitional range, and 25–900 °C – to the brittle range (Fig. 3).

Fractography

After tensile tests, the fractures of the samples were examined at temperatures corresponding to the brittle (700 °C), transition (950 °C) and ductile (1000 °C) ranges. After stretching at *T*=700 °C, the fracture is predominantly intercrystallite (Fig. 4 a). The fracture surface is predominantly represented by flat cleavage facets along the α_2/γ interphase boundaries with an orientation close to 75–90° relative to the tensile axis, as well as along the colony boundaries (Fig. 4 a). After testing at *T*=950 °C, traces of the propagation of tortuous cracks are visible on the fracture, the fracture becomes transcrystalline, and the number of secondary cracks increases (Fig. 4 b). The facets are no longer absolutely smooth, while the main area of the fracture is still represented by brittle cleaved areas along the interphase boundaries. It is worth noting the absence of areas indicating fracture along the α_2/γ interphase boundaries, which indicates branching of the main crack inside the colonies. Cardinal changes occur at a temperature of 1000 °C (Fig. 4 c). At low magnification, the fracture looks like a dimple; a more detailed study of the fracture surface confirms the presence of dimples. It is worth noting that spherical formations arising on the fracture surface during localisation of deformation and dynamic recrystallisation/spheroidisation are observed on the fracture surface (Fig. 4 c). Oxidation at *T*=1000 °C of the dimple edges characteristic of the viscous type of fracture can lead to the formation of oxidised spherical formations (Fig. 4 c). The share of the viscous component of the fracture was 70 % (Fig. 4 c).

Changes in microstructure after deformation in the fracture zone

To study crack propagation and microstructure evolution in more detail, during testing, polished side surfaces of samples in fracture zones after tension were examined (Fig. 5). At *T*=700 °C, propagation of main and secondary cracks is observed both along colony boundaries and along α_2/γ interphase boundaries (Fig. 5 a). The length of secondary cracks does not exceed 100 μm. Signs of hindered movement of secondary cracks in favourably oriented ($15<\Phi<75°$) lamellar colonies are clearly visible, causing the formation of bridges in the colony body (Fig. 5 a) or the formation of new cracks along colony boundaries, where their propagation is less hindered (Fig. 5 a). Unfavourably oriented ($\Phi<15°$ and $\Phi>75°$) colonies are significantly less involved in plastic deformation; cracks propagate along α_2/γ boundaries or along colony boundaries (Fig. 5 a). An increase in the deformation temperature to 950 °C leads to a more active formation of secondary cracks and the formation of bridges even in the case of unfavourably oriented colonies (Fig. 5 b). It is worth noting the complete dissolution of the ω-phase particles at a temperature of 950 °C and an increase in the volume fraction of the β-phase to 15 % due to the formation of particles 0.1–3 μm in size in the body of the lamellar colonies (Fig. 5 b). Fundamental changes are observed upon reaching a temperature of 1000 °C (Fig. 5 c). Active formation of new pores is observed mainly along the colony boundaries, while in unfavourably oriented colonies, cracks form along the α_2/γ interphase boundaries, and in the case of favourably oriented colonies, bending of the plates occurs (Fig. 5 c). Spherical/polygonal particles of the $\gamma/\alpha_2/\beta$-phases 0.1–3 μm in size are predominantly located along the colony boundaries (Fig. 5 c). It is evident that small pores are formed along the boundaries and in the body of the colonies along the chains of β-phase particles (Fig. 5 c). Moreover, large pores are predominantly located at the boundaries of favourably and unfavourably oriented colonies (Fig. 5 c). The volume fraction of pores near the fracture zone reaches 12 % (Fig. 5 c).

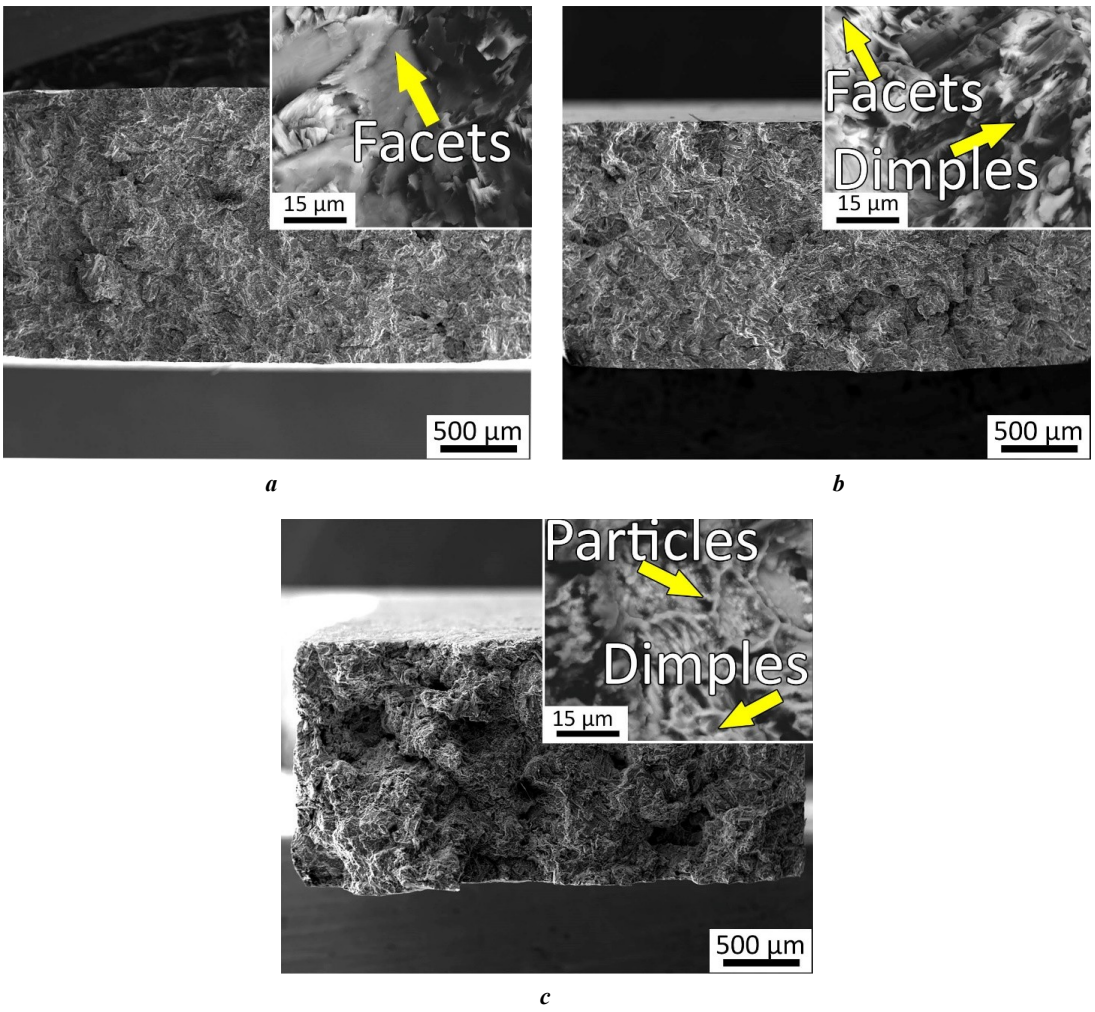

a *b*

c

Fig. 4. *Fractures of samples after tensile tests of cast TNM-B1 alloy:*
a *– 700 °C;* ***b*** *– 950 °C;* ***c*** *– 1000 °C.*
In the enlarged areas of the fractures, facets, dimples and particles are visible
Рис. 4. *Изломы образцов после испытаний на растяжение литого сплава TNM-B1:*
a *– 700 °C;* ***b*** *– 950 °C;* ***c*** *– 1000 °C.*
На увеличенных участках изломов видны фасетки, ямки и частицы

DISCUSSION

The obtained results showed a significant effect of temperature on the mechanical properties of the TNM-B1 alloy, its phase composition and changes in the fracture pattern in colonies with different orientations relative to the deformation axis. Three temperature ranges corresponding to brittle (25–900 °C), transition (950 °C) and ductile (1000 °C) behaviour of the alloy were found. The lamellar type of microstructure, the presence of γ-phase particles, interlayers of β(B2)+ω-phases and borides along the colony boundaries greatly limited the plasticity of the alloy in a wide temperature range. According to [13], at temperatures above 850 °C, the ω-phase particles dissolve, which did not have a noticeable effect on the plasticity level, as a result of which the fracture pattern was predominantly of the intercrystallite type of fracture. Plastic deformation was localised and manifested itself in the formation of bridges in favourably oriented colonies below the temperature of the brittle-ductile transition (Fig. 5 a), which is associated with limited plasticity only in colonies with an orientation of $15<\Phi<75°$ [12]. In the case of unfavourably oriented colonies, the stress level did not reach the values necessary for the plastic deformation onset, which led to the propagation of cracks mainly along the α_2/γ interphase boundaries (Fig. 5 a). This behaviour is associated with the mechanical behaviour anisotropy of colonies with different orientations relative to the deformation axis [8; 9; 12]. According to [10], an increase in the deformation temperature to 950 °C led to the activation of multiple slip and an increase in diffusion, which was expressed in a change in the fracture type from intercrystallite to transcrystalline, the appearance of dimples and the formation of bridges regardless of the orientation of the colonies relative to the deformation axis (Fig. 5). With further increase in temperature, spheroidisation/recrystallisation is activated, which leads to softening and increased plasticity [14]. The formation of new dispersed β-phase particles upon heating to 950–1000 °C is an expected consequence of the increase in the equilibrium β-phase content in the alloy [15], which is typical for TNM alloys when held in the range of 900–1100 °C [15]. As was

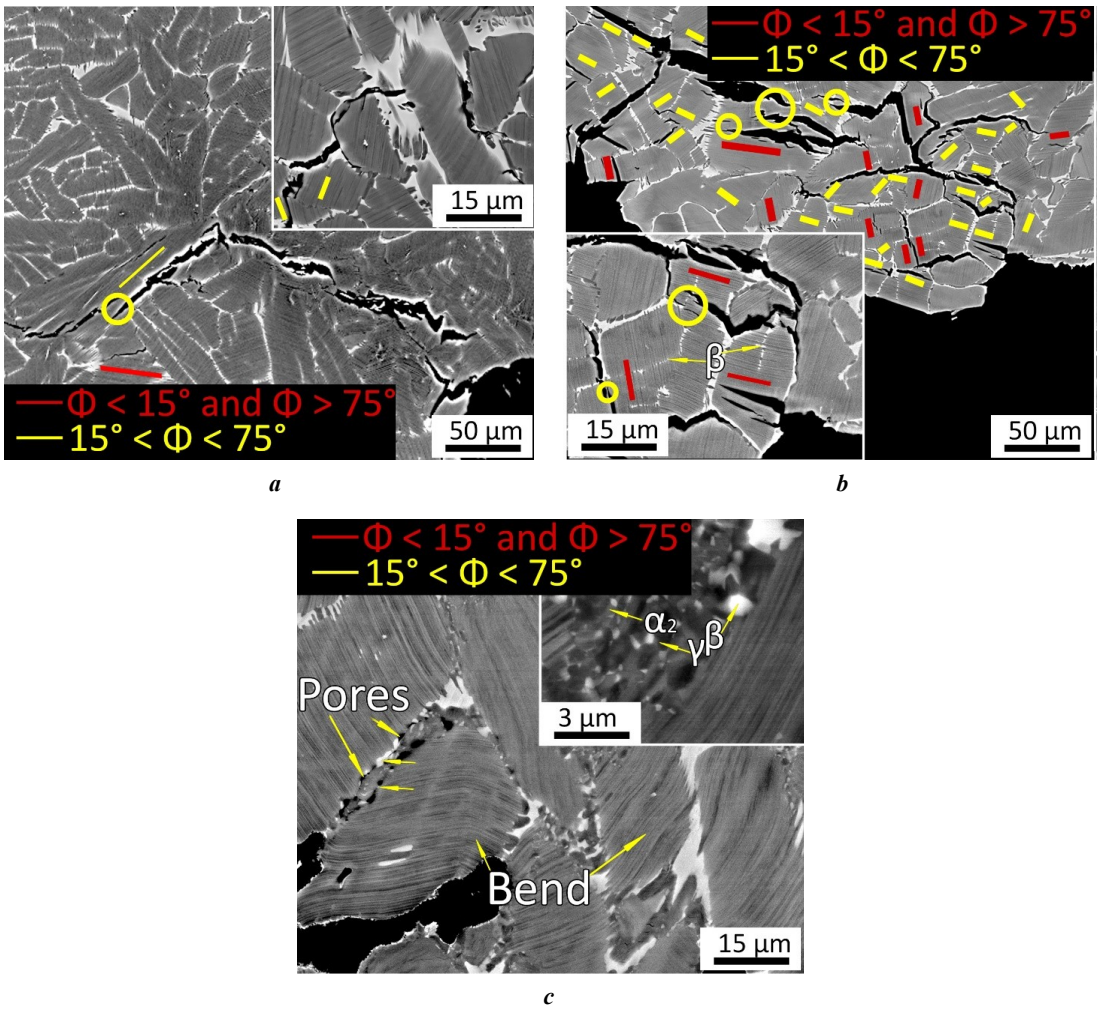

Fig. 5. *Microstructure of samples after tensile tests near the fracture zone:*
a *– 700 °C;* ***b*** *– 950 °C;* ***c*** *– 1000 °C.*
The tensile axis is vertical. The circles indicate the bridges. The arrows indicate the structural elements. The yellow and red lines indicate the colonies favorably and unfavorably oriented relative to the deformation axis, respectively
Рис. 5. *Микроструктура образцов после испытаний на растяжение вблизи зоны разрушения:*
a *– 700 °C;* ***b*** *– 950 °C;* ***c*** *– 1000 °C.*
Ось растяжения расположена вертикально. Окружностями обозначены перемычки. Стрелками обозначены структурные элементы. Желтыми и красными линиями обозначены благоприятно и неблагоприятно ориентированные относительно оси деформации колонии соответственно

shown (Fig. 5), small pores were formed predominantly at the β/γ boundaries, which is consistent with the data [16]. Their formation can be provoked by a higher coefficient of thermal expansion of the β-phase in relation to the γ-phase, leading to local thermal stresses [17].

Particular attention should be paid to the observed mechanism of bridge formation during crack growth. They are formed as a result of plastic deformation between adjacent areas, and their presence correlates with fracture toughness, since it is associated with the work of plastic deformation in the crack propagation zone [18]. The formation of bridges in colonies with different orientations relative to the deformation axis can be affected by microstructural parameters, as well as fracture toughness, which was shown in [18]. Fracture toughness increases with increasing colony size due to the tendency to form larger bridges [19; 20]. As shown in [21], saturation is observed for colonies larger than 600 μm, which can be partly associated with the large colony size, since in such cases only a few colonies are encountered along the crack propagation path. An increase in fracture toughness with a decrease in the interlamellar distance is associated with a hindrance to translamellar cracking, which leads to an increase in the number of bridges [18], a decrease in the interlamellar distance of less than 100 nm leads to the intercrystallite type of fracture due to a decrease in ductility. On the contrary, thick lamellae promote translamellar cracking and facilitated connection of microcracks with the main crack, which leads to the formation of a smaller number of smaller bridges and a decrease in fracture toughness [18]. Previous results [8] confirm those obtained in this work, namely, the formation of bridges only in favourably oriented colonies at room

temperature in the alloy with λ~100 nm and a decrease in their number at λ~10 nm, as well as the predominance of translamellar cracking at λ~800 nm. Most likely, an increase in the colony size will not lead to a change in crack propagation in colonies with different orientations relative to the tensile axis.

The obtained results show that an increase in temperature leads to a change in the phase composition, dissolution of embrittling particles and the development of spheroidisation/recrystallisation, which leads to a change in the behaviour of the alloy from brittle to ductile. The orientation of the lamellae relative to the tensile axis fundamentally affects crack propagation. In the temperature range corresponding to brittle fracture, bridges were formed only in the case of favourable colony orientation; when transition and viscous fracture were reached, bridges were formed regardless of orientation.

CONCLUSIONS

1. The microstructure of the cast TNM-B1 alloy was studied. It was represented mainly by (α_2+γ)-plate colonies with interlayers of a mixture of β(B2)+ω-phases located along the boundaries. At deformation temperatures above 950 °C, dissolution of ω-phase particles and precipitation of dispersed particles of the secondary β-phase were identified.

2. The effect of tensile deformation temperature on mechanical properties was considered. With an increase in deformation temperature, a continuous increase in relative elongation was observed, reaching a maximum of δ=22.5 % at T=1000 °C, and a nonlinear change in strength with a maximum of σ_B=592 MPa at T=800 °C, followed by a decrease to σ_B=340 MPa at T=1000 °C. The fracture pattern was predominantly intercrystallite in the brittle, transcrystalline in the transition, and dimple in the ductile temperature range of deformation. The brittle-ductile transition corresponded to a temperature range of about 950 °C, which corresponded to the transition state of the alloy.

3. A study was conducted to investigate the effect of temperature on crack propagation in the alloy structure. A different pattern of crack propagation was found in favourably and unfavourably oriented colonies relative to the deformation axis, which was expressed in the inhibition of crack propagation and the formation of bridges in favourably oriented colonies, in contrast to unfavourably oriented ones. An increase in temperature to 950 °C resulted in no difference in the pattern of crack propagation in colonies with different orientations relative to the axis of tension. When the temperature reached 1000 °C, no cracks were observed, as well as the formation of pores along the boundaries of colonies and along the chains of secondary β-phase particles.

REFERENCES

1. Genc O., Unal R. Development of gamma titanium aluminide (γ-TiAl) alloys: A review. *Journal of Alloys and Compounds*, 2022, vol. 929, article number 167262. DOI: 10.1016/j.jallcom.2022.167262.
2. Duan Baohua, Yang Yuchen, He Shiyu et al. History and development of γ-TiAl alloys and the effect of alloying elements on their phase transformations. *Journal of Alloys and Compounds*, 2022, vol. 909, article number 164811. DOI: 10.1016/j.jallcom.2022.164811.
3. Musi M., Graf G., Clemens H., Spoerk-Erdely P. Alloying elements in intermetallic γ-TiAl based alloys – A review on their influence on phase equilibria and phase transformations. *Advanced Engineering Materials*, 2024, vol. 26, no. 4, article number 2300610. DOI: 10.1002/adem.202300610.
4. Tetsui T., Fukuyo T., Mizuta K. Comparison of the impact resistance of TiAl4822 and TNM alloy under expected service conditions of jet engine blades. *Intermetallics*, 2025, vol. 183, article number 108793. DOI: 10.1016/j.intermet.2025.108793.
5. Imayev R.M., Kaibyshev O.A., Salishchev G.A. Mechanical behaviour of fine grained TiAl intermetallic compound II. Ductile-brittle transition. *Acta Metallurgica Materialia*, 1992, vol. 40, no. 3, pp. 589–595. DOI: 10.1016/0956-7151(92)90408-7.
6. Wu Hao, Zhang Yida, Lu Dong, Gong Xiufang, Lei Liming, Zhang Hong, Liu Yongjie, Wang Qingyuan. Exploring the brittle-to-ductile transition and microstructural responses of TiAl alloy with a crystal plasticity model incorporating dislocation and twinning. *Materials & Design*, 2024, vol. 246, article number 113360. DOI: 10.1016/j.matdes.2024.113360.
7. Appel F., Lorenz U., Oehring M., Sparka U., Wagner R. Thermally activated deformation mechanisms in microalloyed two-phase titanium aluminide alloys. *Materials Science and Engineering: A*, 1997, vol. 233, no. 1-2, pp. 1–14. DOI: 10.1016/S0921-5093(97)00043-9.
8. Panov D.O., Sokolovsky V.S., Stepanov N.D., Zherebtsov S.V., Panin P.V., Volokitina E.I., Nochovnaya N.A., Salishchev G.A. Effect of interlamellar spacing on strength-ductility combination of β-solidified γ-TiAl based alloy with fully lamellar structure. *Materials Science and Engineering: A*, 2023, vol. 862, article number 144458. DOI: 10.1016/j.msea.2022.144458.
9. Hu D., Loretto M.H. Slip transfer between lamellae in fully lamellar TiAl alloys. *Intermetallics*, 1999, vol. 7, no. 11, pp. 1299–1306. DOI: 10.1016/S0966-9795(99)00049-7.
10. Mishin Y., Herzig Ch. Diffusion in the Ti–Al system. *Acta Materialia*, 2000, vol. 48, no 3, pp. 589–623. DOI: 10.1016/S1359-6454(99)00400-0.
11. Liu Xin, Liu Hongguang, Shi Shijia, Tang Yuyang, Zhang Jun. On revealing the mechanisms involved in brittle-to-ductile transition of fracture behaviors for γ-TiAl alloy under dynamic conditions. *Journal of Alloys and Compounds*, 2025, vol. 1010, article number 177614. DOI: 10.1016/j.jallcom.2024.177614.
12. Edwards T.E.J., Di Gioacchino F., Goodfellow A.J., Mohanty G., Wehrs J., Michler J., Clegg W.J. Deformation of lamellar γ-TiAl below the general yield stress. *Acta Materialia*, 2019, vol. 163, pp. 122–139. DOI: 10.1016/j.actamat.2018.09.061.
13. Schloffer M., Rashkova B., Schöberl T., Schwaighofer E., Zhang Zhang, Clemens H., Mayer S. Evolution of the ω_o phase in a β-stabilized multi-phase TiAl alloy and

its effect on hardness. *Acta Materialia*, 2014, vol. 64, pp. 241–252. DOI: 10.1016/j.actamat.2013.10.036.
14. Molenat G., Galy B., Musi M., Toualbi L., Thomas M., Clemens H., Monchoux J.Ph., Couret A. Plasticity and brittleness of the ordered β_o phase in a TNM-TiAl alloy. *Intermetallics*, 2022, vol. 151, article number 107653. DOI: 10.1016/j.intermet.2022.107653.
15. Kuznetsov A.V., Sokolovskii V.S., Salishchev G.A., Belov N.A., Nochovnaya N.A. Thermodynamic modeling and experimental study of phase transformations in alloys based on γ-TiAl. *Metal Science and Heat Treatment*, 2016, vol. 58, pp. 259–267. DOI: 10.1007/s11041-016-9999-2.
16. Zhu Bin, Xue Xiangyi, Kou Hongchao, Li Xiaolei, Li Jinshan. The cavitation of high Nb-containing TiAl alloys during tensile tests around BDTT. *Materials Science and Engineering: A*, 2018, vol. 729, pp. 86–93. DOI: 10.1016/j.msea.2018.05.028.
17. Staron P., Stark A., Schell N., Spoerk-Erdely P., Clemens H. Thermal expansion of a multiphase intermetallic Ti-Al-Nb-Mo alloy studied by high-energy X-ray diffraction. *Materials*, 2021, vol. 14, no. 4, article number 727. DOI: 10.3390/ma14040727.
18. Kim Y.W. Effects of microstructure on the deformation and fracture of γ-TiAl alloys. *Materials Science and Engineering: A*, 1995, vol. 192-193, part 2, pp. 519–533. DOI: 10.1016/0921-5093(94)03271-8.
19. Liu C.T., Schneibel J.H., Maziasz P.J., Wright J.L., Easton D.S. Tensile properties and fracture toughness of TiAl alloys with controlled microstructures. *Intermetallics*, 1996, vol. 4, no. 6, pp. 429–440. DOI: 10.1016/0966-9795(96)00047-7.
20. Wang J.N., Xie K. Refining of coarse lamellar microstructure of TiAl alloys by rapid heat treatment. *Intermetallics*, 2000, vol. 8, no. 5-6, pp. 545–548. DOI: 10.1016/S0966-9795(99)00153-3.
21. Rogers N.J., Crofts P.D., Jones I.P., Bowen P. Microstructure toughness relationships in fully lamellar γ-based titanium aluminides. *Materials Science and Engineering: A*, 1995, vol. 192-193, part 1, pp. 379–386. DOI: 10.1016/0921-5093(94)03222-X.

СПИСОК ЛИТЕРАТУРЫ

1. Genc O., Unal R. Development of gamma titanium aluminide (γ-TiAl) alloys: A review // Journal of Alloys and Compounds. 2022. Vol. 929. Article number 167262. DOI: 10.1016/j.jallcom.2022.167262.
2. Duan Baohua, Yang Yuchen, He Shiyu et al. History and development of γ-TiAl alloys and the effect of alloying elements on their phase transformations // Journal of Alloys and Compounds. 2022. Vol. 909. Article number 164811. DOI: 10.1016/j.jallcom.2022.164811.
3. Musi M., Graf G., Clemens H., Spoerk-Erdely P. Alloying elements in intermetallic γ-TiAl based alloys – A review on their influence on phase equilibria and phase transformations // Advanced Engineering Materials. 2024. Vol. 26. № 4. Article number 2300610. DOI: 10.1002/adem.202300610.
4. Tetsui T., Fukuyo T., Mizuta K. Comparison of the impact resistance of TiAl4822 and TNM alloy under expected service conditions of jet engine blades // Intermetallics. 2025. Vol. 183. Article number 108793. DOI: 10.1016/j.intermet.2025.108793.
5. Imayev R.M., Kaibyshev O.A., Salishchev G.A. Mechanical behaviour of fine grained TiAl intermetallic compound II. Ductile-brittle transition // Acta Metallurgica Materialia. 1992. Vol. 40. № 3. P. 589–595. DOI: 10.1016/0956-7151(92)90408-7.
6. Wu Hao, Zhang Yida, Lu Dong, Gong Xiufang, Lei Liming, Zhang Hong, Liu Yongjie, Wang Qingyuan. Exploring the brittle-to-ductile transition and microstructural responses of TiAl alloy with a crystal plasticity model incorporating dislocation and twinning // Materials & Design. 2024. Vol. 246. Article number 113360. DOI: 10.1016/j.matdes.2024.113360.
7. Appel F., Lorenz U., Oehring M., Sparka U., Wagner R. Thermally activated deformation mechanisms in microalloyed two-phase titanium aluminide alloys // Materials Science and Engineering: A. 1997. Vol. 233. № 1-2. P. 1–14. DOI: 10.1016/S0921-5093(97)00043-9.
8. Panov D.O., Sokolovsky V.S., Stepanov N.D., Zherebtsov S.V., Panin P.V., Volokitina E.I., Nochovnaya N.A., Salishchev G.A. Effect of interlamellar spacing on strength-ductility combination of β-solidified γ-TiAl based alloy with fully lamellar structure // Materials Science and Engineering: A. 2023. Vol. 862. Article number 144458. DOI: 10.1016/j.msea.2022.144458.
9. Hu D., Loretto M.H. Slip transfer between lamellae in fully lamellar TiAl alloys // Intermetallics. 1999. Vol. 7. № 11. P. 1299–1306. DOI: 10.1016/S0966-9795(99)00049-7.
10. Mishin Y., Herzig Ch. Diffusion in the Ti–Al system // Acta Materialia. 2000. Vol. 48. № 3. P. 589–623. DOI: 10.1016/S1359-6454(99)00400-0.
11. Liu Xin, Liu Hongguang, Shi Shijia, Tang Yuyang, Zhang Jun. On revealing the mechanisms involved in brittle-to-ductile transition of fracture behaviors for γ-TiAl alloy under dynamic conditions // Journal of Alloys and Compounds. 2025. Vol. 1010. Article number 177614. DOI: 10.1016/j.jallcom.2024.177614.
12. Edwards T.E.J., Di Gioacchino F., Goodfellow A.J., Mohanty G., Wehrs J., Michler J., Clegg W.J. Deformation of lamellar γ-TiAl below the general yield stress // Acta Materialia. 2019. Vol. 163. P. 122–139. DOI: 10.1016/j.actamat.2018.09.061.
13. Schloffer M., Rashkova B., Schöberl T., Schwaighofer E., Zhang Zhang, Clemens H., Mayer S. Evolution of the ω_o phase in a β-stabilized multi-phase TiAl alloy and its effect on hardness // Acta Materialia. 2014. Vol. 64. P. 241–252. DOI: 10.1016/j.actamat.2013.10.036.
14. Molenat G., Galy B., Musi M., Toualbi L., Thomas M., Clemens H., Monchoux J.Ph., Couret A. Plasticity and brittleness of the ordered β_o phase in a TNM-TiAl alloy // Intermetallics. 2022. Vol. 151. Article number 107653. DOI: 10.1016/j.intermet.2022.107653.
15. Kuznetsov A.V., Sokolovskii V.S., Salishchev G.A., Belov N.A., Nochovnaya N.A. Thermodynamic modeling and experimental study of phase transformations in alloys based on γ-TiAl // Metal Science and Heat Treatment. 2016. Vol. 58. P. 259–267. DOI: 10.1007/s11041-016-9999-2.
16. Zhu Bin, Xue Xiangyi, Kou Hongchao, Li Xiaolei, Li Jinshan. The cavitation of high Nb-containing TiAl

alloys during tensile tests around BDTT // Materials Science and Engineering: A. 2018. Vol. 729. P. 86–93. DOI: 10.1016/j.msea.2018.05.028.
17. Staron P., Stark A., Schell N., Spoerk-Erdely P., Clemens H. Thermal expansion of a multiphase intermetallic Ti-Al-Nb-Mo alloy studied by high-energy X-ray diffraction // Materials. 2021. Vol. 14. № 4. Article number 727. DOI: 10.3390/ma14040727.
18. Kim Y.W. Effects of microstructure on the deformation and fracture of γ-TiAl alloys // Materials Science and Engineering: A. 1995. Vol. 192-193. Part 2. P. 519–533. DOI: 10.1016/0921-5093(94)03271-8.
19. Liu C.T., Schneibel J.H., Maziasz P.J., Wright J.L., Easton D.S. Tensile properties and fracture toughness of TiAl alloys with controlled microstructures // Intermetallics. 1996. Vol. 4. № 6. P. 429–440. DOI: 10.1016/0966-9795(96)00047-7.
20. Wang J.N., Xie K. Refining of coarse lamellar microstructure of TiAl alloys by rapid heat treatment // Intermetallics. 2000. Vol. 8. № 5-6. P. 545–548. DOI: 10.1016/S0966-9795(99)00153-3.
21. Rogers N.J., Crofts P.D., Jones I.P., Bowen P. Microstructure toughness relationships in fully lamellar γ-based titanium aluminides // Materials Science and Engineering: A. 1995. Vol. 192-193. Part 1. P. 379–386. DOI: 10.1016/0921-5093(94)03222-X.

УДК 669.017.165
doi: 10.18323/2782-4039-2025-3-73-6

Исследование влияния температуры деформации на механическое поведение и особенности разрушения литого сплава TNM-B1

Соколовский Виталий Сергеевич*, кандидат технических наук,
научный сотрудник лаборатории объемных наноструктурных материалов
Салищев Геннадий Алексеевич[1], доктор технических наук, профессор,
заведующий лабораторией объемных наноструктурных материалов
Белгородский государственный национальный исследовательский университет, Белгород (Россия)

***E-mail:** sokolovskiy@bsuedu.ru [1]ORCID: https://orcid.org/0000-0002-0815-3525

Поступила в редакцию 07.07.2025 *Пересмотрена 25.07.2025* *Принята к публикации 20.08.2025*

Аннотация: Статья посвящена β-затвердевающим сплавам на основе TiAl, которые являются крайне перспективными для авиационной промышленности материалами с рабочей температурой до 850 °C, обладают высокими удельными прочностными характеристиками. Исследовано влияние температуры деформации при растяжении в интервале *T*=25–1000 °C на механические свойства, фазовый состав и трещинообразование в литом сплаве – β-затвердевающем TNM-B1. Установлено, что литой сплав TNM-B1 характеризуется комплексной микроструктурой, включающей (α_2+γ)-пластинчатые колонии и прослойки β(B2)+ω-фаз, эволюция которых при повышенных температурах деформации определяет поведение материала. Показано, что растворение ω-фазы и выделение дисперсных частиц вторичной β-фазы при *T*>950 °C оказывают существенное влияние на механические характеристики. Установлена выраженная температурная зависимость прочности и пластичности: максимальная прочность наблюдается при 800 °C, в то время как наибольшее относительное удлинение в исследованном интервале температур достигается при 1000 °C. Переход от хрупкого к вязкому характеру разрушения происходит в интервале температур в области 950 °C. Кроме того, выявлена зависимость механизма распространения трещин от ориентации пластинчатых колоний относительно оси деформации: при повышении температуры различия нивелируются, а при 1000 °C наблюдается полное подавление трещинообразования с формированием пор вдоль границ колоний и скоплений частиц вторичной β-фазы. Полученные результаты демонстрируют важную роль микроструктурных превращений в формировании деформационного поведения и механических свойств сплава на основе гамма-алюминида титана TNM-B1, что имеет практическое значение для разработки технологий его термомеханической обработки.

Ключевые слова: литой сплав TNM-B1; механическое поведение; особенности разрушения; сплав типа TNM; микроструктура; хрупко-вязкий переход; прочность; пластичность.

Благодарности: Работа выполнена при финансовой поддержке Российского научного фонда (соглашение № 19-79-30066) с использованием оборудования Центра коллективного пользования «Технологии и материалы» НИУ «БелГУ», https://rscf.ru/prjcard_int?19-79-30066.

Для цитирования: Соколовский В.С., Салищев Г.А. Исследование влияния температуры деформации на механическое поведение и особенности разрушения литого сплава TNM-B1 // Frontier Materials & Technologies. 2025. № 3. С. 81–89. DOI: 10.18323/2782-4039-2025-3-73-6.